

Electronic Supplementary Information

Materials and methods

General details: All the reactions were carried out under inert atmosphere, unless otherwise stated. Solvents used for various reactions were dried using a commercial solvent purification/drying system. Solvents used for extractions and column chromatography, and all other reagents were used as supplied by commercial vendors without further purifications or drying. Compounds 2,2',7,7'-tetrabromospiro[fluorene-9,9'-xanthene] and 2,5-Bis(2-ethylhexyl)-3-(5-(4,4,5,5-tetramethyl-1,3,2-dioxaborolan-2-yl)thiophen-2-yl)-2,5-dihydropyrrolo[3,4-c]pyrrole-1,4-dione were purchased from SunaTech Incorporation, China and were used as received.

Thin layer chromatography (TLC) was performed using 0.25 mm thick plates pre-coated with Merck Kieselgel 60 F₂₅₄ silica gel and visualized using UV light (254 and 365 nm). Petroleum spirits with a boiling point range of 40–60 °C were used wherever indicated. Column chromatography was performed on either 40–60 or 20–40 microns silica gel. ¹H NMR spectra were recorded at 300, 400 or 500 MHz as indicated. The following abbreviations were used to explain multiplicities: s = singlet, d = doublet, t = triplet, q = quartet, m = multiplet, br = broad, dd = doublet of doublets, and dt = doublet of triplets. ¹³C NMR spectra were recorded at 75 or 101 MHz as indicated. ¹H and ¹³C chemical shifts were calibrated using residual non-deuterated solvent as an internal reference and are reported in parts per million (δ) relative to tetramethylsilane ($\delta = 0$). PESA measurements were recorded using a Riken Keiki AC-2 PESA spectrometer with a power setting of 5 nW and a power number of 0.5. Samples for PESA were prepared on cleaned glass substrates. Electrochemical measurements were carried out using a PowerLab ML160 potentiostat interfaced *via* a PowerLab 4/20 controller to a PC running E-Chem For Windows version 1.5.2. The measurements were run in argon-purged dichloromethane with tetrabutylammonium hexafluorophosphate (0.1 M) as the supporting electrolyte. The cyclic voltammograms were recorded using a standard three electrode configuration with a glassy carbon (2 mm diameter) working electrode, a platinum wire counter electrode and a silver wire pseudo reference electrode. The silver wire was cleaned in concentrated nitric acid followed by concentrated hydrochloric acid and then washed with deionised water. Cyclic-voltammograms were recorded with a sweep rate of 50 mV per second. All the potentials were referred to the E_{1/2} of ferrocene/ferrocenium redox couple. Differential scanning calorimetry (DSC) experiments were carried out using Q-100 DSC instrument with nitrogen as a purging gas. Samples were heated to 250 °C at a heating rate of 10 °C per minute. Thermogravimetric analysis (TGA) experiments were conducted using Q-500 TGA instrument with nitrogen as a purging gas. Samples were heated to 900 °C at a rate of 10 °C/minute under nitrogen atmosphere. Atomic force microscopy (AFM) topographic maps were directly performed on the active layers of SFX1 blends using an Asylum Research MFP-3D-SA instrument. The AFM was run in intermittent contact mode (tapping mode) using

MicroMasch NSC18 tips (typical resonant frequency \sim 100 kHz, typical probe radius \sim 10 nm and typical aspect ratio 3: 1). TEM samples were prepared on a holey carbon grid and the micrographs were produced using a JOEL 1010 100 kV TEM.

Device fabrication and characterization of photovoltaic devices: Indium tin oxide (ITO)-coated glass (Kintek, 15 Ohms per square) was cleaned by standing in a stirred solution of 5% (v/v) Deconex 12PA detergent at 90 °C for 20 min. The ITO-coated glass was then successively sonicated for 10 min each in distilled water, acetone and isopropanol. The substrates were then exposed to a UV–ozone clean at room temperature for 10 min. UV/ozone cleaning of glass substrates was performed using a Novascan PDS-UVT, UV/ozone cleaner with the platform set to maximum height. The intensity of the lamp was greater than 36 mW/cm² at a distance of 10 cm. At ambient conditions the ozone output of the UV cleaner is greater than 50 ppm. Aqueous solutions of PEDOT/PSS (HC Starck, Baytron P Al 4083) were filtered (0.2 μ m RC filter) and deposited onto glass substrates in air by spin coating (Laurell WS-400B-6NPP lite single wafer spin processor) at 5000 rpm for 60 s to give a layer having a thickness of 40 \pm 5 nm. The PEDOT/PSS layer was then annealed on a hotplate in a glove box at 145 °C for 10 min. For OPV devices, the newly synthesized SFX1 and donor polymers were dissolved in individual vials by magnetic stirring. Blend ratios and solution concentrations were varied to optimize device performance. The solutions were then combined, filtered (0.2 μ m RC filter) and deposited by spin coating onto the ITO-coated glass substrates inside a glove box. The coated substrates were then transferred (without exposure to air) to a vacuum evaporator inside an adjacent nitrogen-filled glove box. Samples were placed on a shadow mask in a tray. The area defined by the shadow mask gave device areas of exactly 0.2 cm². Deposition rates and film thicknesses were monitored using a calibrated quartz thickness monitor inside the vacuum chamber. Layers of calcium (Ca) (Aldrich) and aluminium (Al) (3 pellets of 99.999%, KJ Lesker) having thicknesses of 20 nm and 100 nm, respectively, were evaporated from open tungsten boats onto the active layer by thermal evaporation at pressures less than 2×10^{-6} mbar. A connection point for the ITO electrode was made by manually scratching off a small area of the active layers. A small amount of silver paint (Silver Print II, GC Electronics, part no.: 22-023) was then deposited onto all of the connection points, both ITO and Al. The completed devices were then encapsulated with glass and a UV-cured epoxy (Summers Optical, Lens Bond type J-91) by exposing to 365 nm UV light inside a glove box for 10 min. The encapsulated devices were then removed from the glove box and tested in air within 1 h. The OPV devices were tested using an Oriel solar simulator fitted with a 1000 W xenon lamp filtered to give an output of 100 mW/cm² at simulated AM1.5. The lamp was calibrated using a standard, filtered silicon (Si) cell from Peccell Limited which was subsequently cross-calibrated with a standard reference cell traceable to the National Renewable Energy Laboratory. The devices were tested using a Keithley 2400 Source meter controlled by lab view software. Film thicknesses were determined using a Dektak 6M Profilometer. The chosen device architecture was simple and well-studied, ITO/PEDOT: PSS (38 nm)/active layer (\sim 75 nm)/Ca (20 nm)/Al (100 nm), where the active layer was a blend of

respective donor and acceptor (**SFX1**). We used *o*-dichlorobenzene as the processing solvent and annealed the blend surfaces at 100 °C for 5 min.

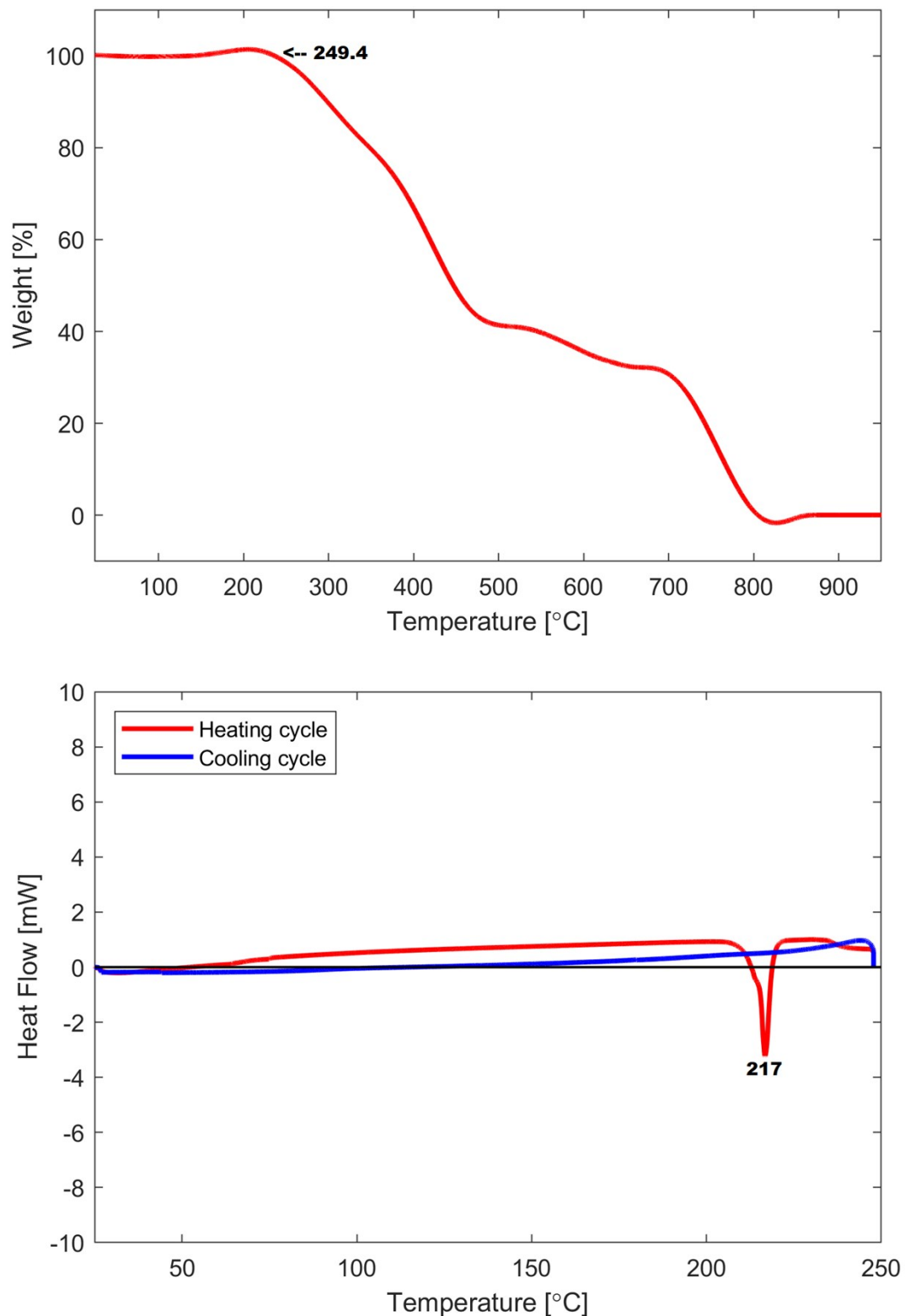


Fig. S1. TGA (above) and DSC (below) curves of SFX1 showing its thermal stability.

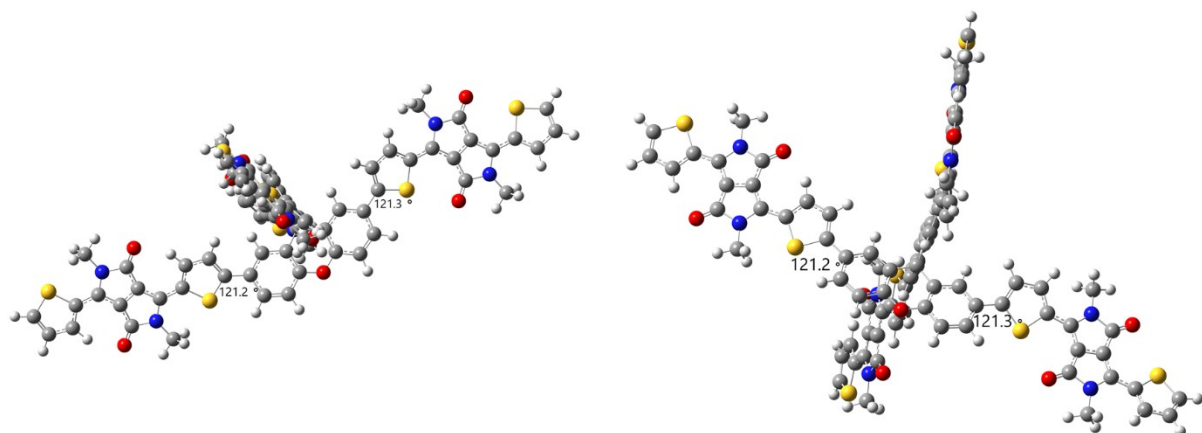


Fig S2. Torsional angle of $\sim 59^\circ$ between the thiophene ring planes (of DPP) and phenyl ring planes (of SFX) of SFX1 from the minimum energy conformations calculated using the Gaussian 09 suite of programs and the B3LYP/6-31G(d) level of theory. [NOTE: Two side views of the molecular format are shown].

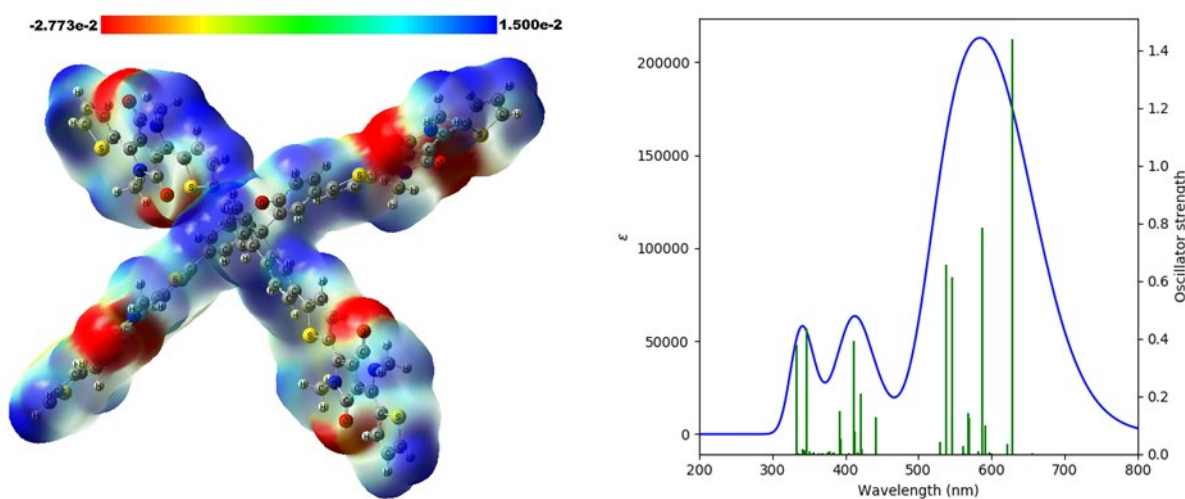


Fig. S3. The molecular electrostatic potential (MEP) map (left) and the computed absorption spectrum (right) of SFX1.

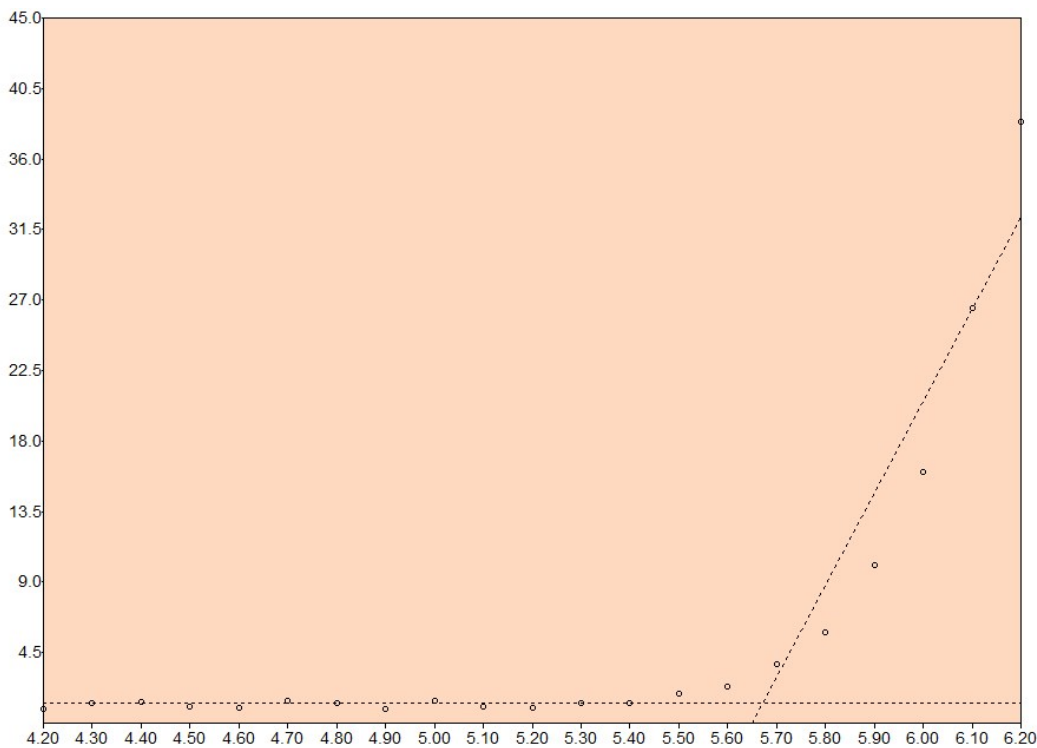


Fig. S4. PESA spectrum of thin film of **SFX1**. The dashed-lines show the fits to extract ionisation potential (-5.67 eV) which corresponds to the HOMO energy level.

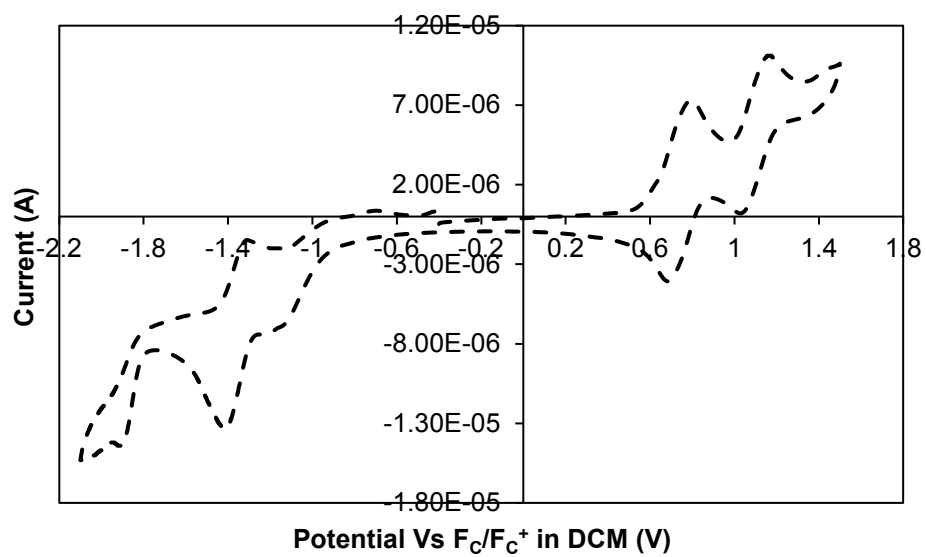


Fig. S5. Cyclic voltammogram of **SFX1**, run in dichloromethane at a sweep rate of 50 mV per second.

Table S1. Photovoltaic cell parameters for **SFX1** blends

Acceptor	Donor	Testing conditions (D: A) ^a	V _{oc} (V)	J _{sc} (mA/cm ²)	FF	Best PCE (%)	Average PCE (%) (\pm std dev) ^f
SFX1	PTB7	1: 1.2 ^b	1.03	14.52 (13.92) ^e	0.63	9.42	9.36 (\pm 0.06)
SFX1	PTB7	1: 1.2 ^c	1.01	11.80 (11.27) ^e	0.61	7.26	7.21 (\pm 0.05)
SFX1	P3HT	1: 1.2 ^b	0.95	11.20 (10.78) ^e	0.61	6.54	6.48 (\pm 0.06)
SFX1	P3HT	1: 1.2 ^c	0.93	10.10 (9.63) ^e	0.60	5.70	5.63 (\pm 0.07)
PC ₆₁ BM	P3HT	1: 1.2 ^d	0.56	8.70 (8.35) ^e	0.63	3.05	3.01 (\pm 0.03)

^a BHJ devices with specified weight ratio. Device structure was ITO/PEDOT: PSS (38 nm)/active layer (~75 nm)/Ca (20 nm)/Al (100 nm); ^b annealed device; ^c unannealed device; ^d A standard P3HT: PC₆₁BM device; ^e integrated values from IPCE spectra; ^f based on ten devices.

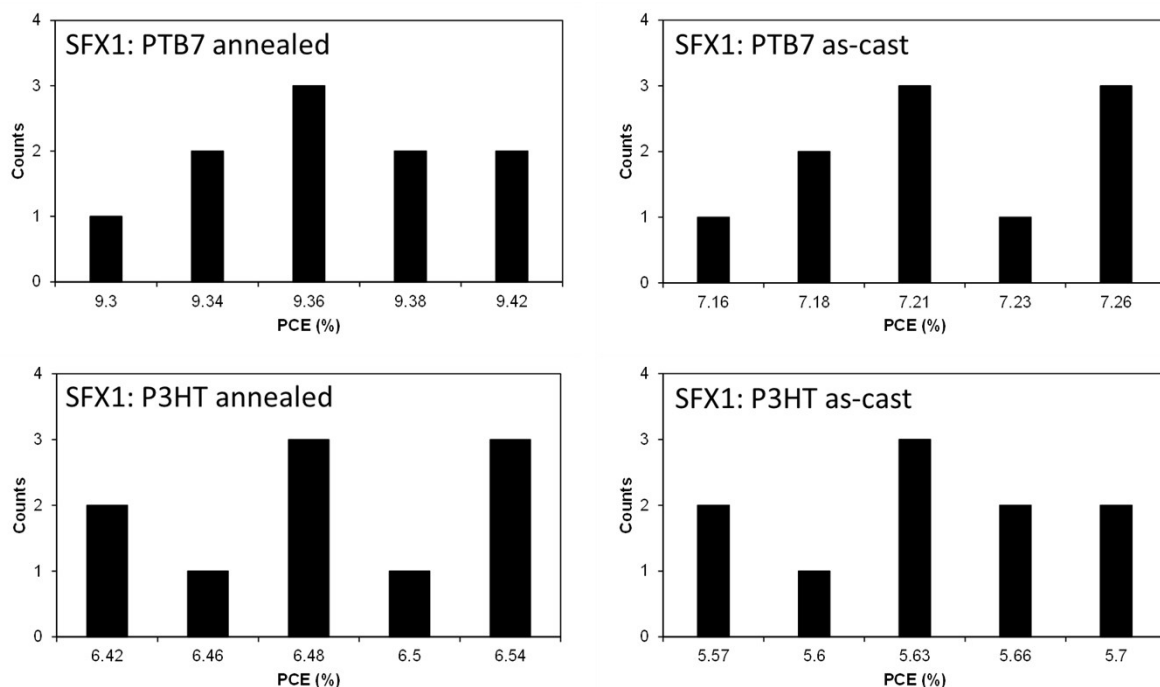


Fig. S6. The distribution curves of devices' efficiency.

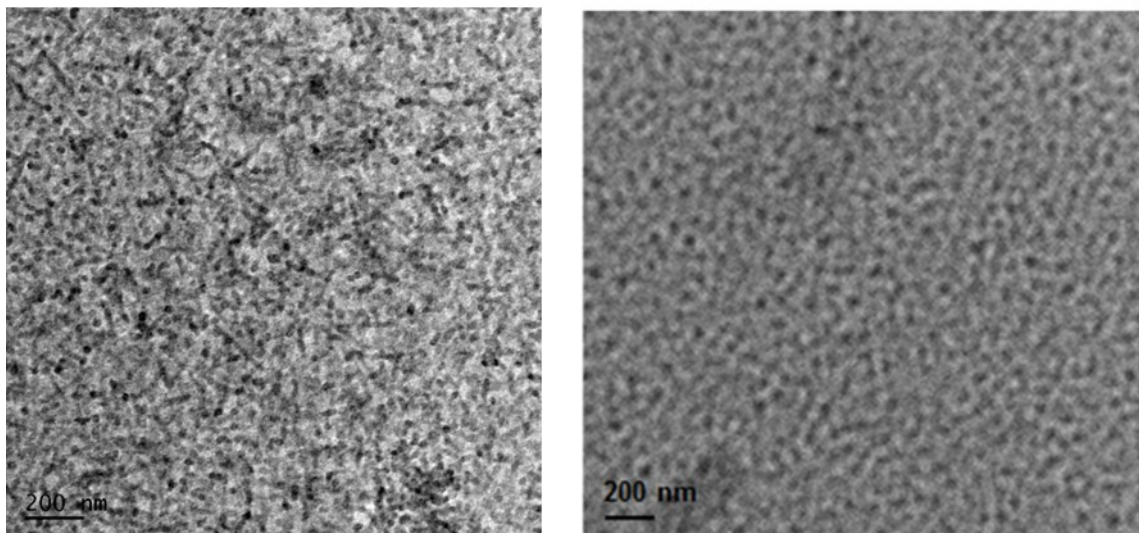


Fig. S7. TEM images for the active blend surfaces of PTB7: **SFX1** (left) and P3HT: **SFX1** (right) (D: A 1: 1.2 w/w). The PTB7 blend surface appeared excellently blended, featureless and fibrous when compared with the P3HT-based blend surface. For a comparative view, identical scale bars of 200 nm are shown.

SCLC details:

To gain an insight into effective charge carrier mobilities, the SCLC method was employed to get information about charge transportation using the electron-only devices. The electron-only devices consisting of an active layer sandwiched between a zinc oxide coated ITO electrode and LiF/Al counter-electrode were fabricated. From the current density as a function of voltage data, the electron mobility in the SCLC region can be estimated using the Mott-Gurney equation, $[J = 9/8 (\varepsilon_0 \varepsilon_r \mu) (V^2/d^3)]$, where J is the current density, $V = V_{\text{applied}} - V_{\text{bi}}$; V_{applied} is the applied potential and V_{bi} is the built-in potential resulting from the work-function difference between two electrodes, ε_r is the dielectric constant of active material, ε_0 is the permittivity of vacuum, μ is the charge carrier mobility, and d is the sample thickness. Using this expression, electron mobilities of the order of 10^{-3} and 10^{-4} were observed for PTB7 and P3HT-based blends [μ_e (PTB7: **SFX1**) = 8.63×10^{-3} cm 2 /Vs; μ_e (P3HT: **SFX1**) = 2.20×10^{-4} cm 2 /Vs], respectively.

Experimental spectra

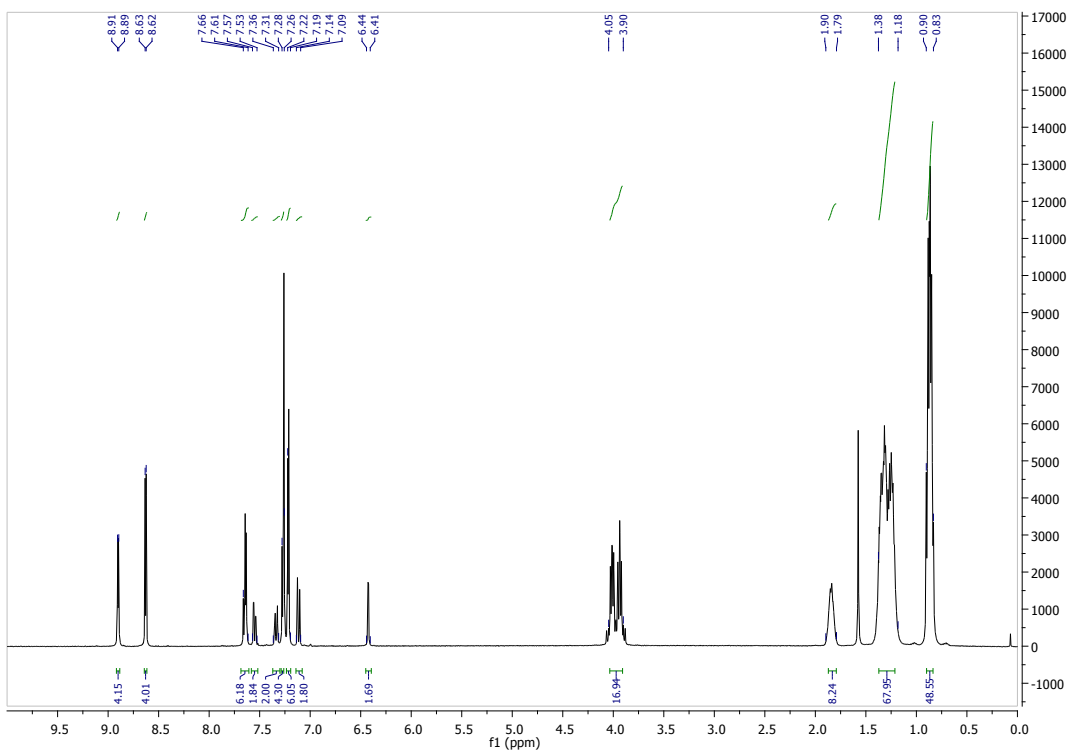


Fig. S8. ^1H NMR spectrum.

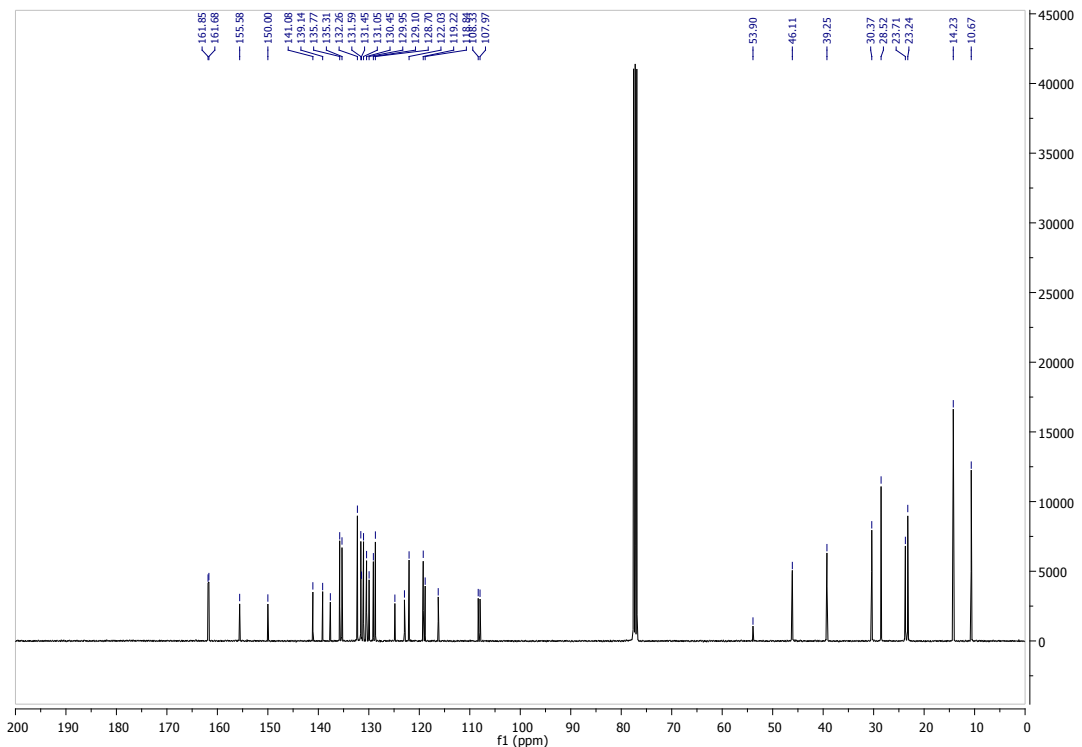


Fig. S9. ^{13}C NMR spectrum.